Numerical Dosimetry at 5G-Bands Using Time-Domain Methods and the Impact of Discretization and Uncertainty in Tissues Constitutive Parameters

Abdelrahman Ijjeh, Soukaina Mifdal, Marylene Cueille, Jean-Lou Dubard, Michel Ney

Numerical Dosimetry at 5G-Bands Using Time-Domain Methods and the Impact of Discretization and Uncertainty in Tissues Constitutive Parameters

Abdelrahman Ijjeh[1], Soukaina Mifdal[1], Marylene Cueille[1], Jean-Lou Dubard[1], Michel Ney[2]
[1] Université Côte d'Azur, CNRS, LEAT, 06903 Sophia Antipolis, France, jean-lou.dubard@univ-cotedazur.fr
[2] IMT Atlantique, Lab-STICC, CS 83818, 29238 Brest Cedex 3, France, michel.ney@imt-atlantique.fr

***Abstract*—Numerical dosimetry is an essential procedure in designing and optimizing propagating EM-devices that confirm to the recommended limits of Specific Absorption Rate (SAR). However, as frequencies go higher, the complexity of the computational problem increases substantially. Moreover, the high heterogeneity of the human body and the uncertainty in its tissues properties add to that complexity. Furthermore, as the numerical domain becomes very large, the impact of numerical dispersion becomes more visible leading to decrease the mesh-size even more. This article sheds some light on the 3D-simulation of such computational problems, and revisits the necessary mesh-size condition that ensures convergence and accuracy of results. Comparisons between FIT and TLM methods are presented to show the speed of convergence for both methods.**

***Index Terms*—Transimssion-Line Matrix (TLM), Finite Integration Technique (FIT), numerical dosimetry, numerical dispersion, Time-Domain (TD) methods, Computational Electromagnetics (CEM), 5G-frequency bands.**

I. INTRODUCTION

Traditionally, in Computational Electromagnetics (CEM) Time-Domain methods it is recommended to use a mesh-size of less than $\lambda/10$, or ten cells per wavelength at most, to ensure a negligible level of numerical dispersion [1] [2]. This limit was derived for a plane wave propagating in a homogeneous medium discretized into a structured homogenous mesh (cubic uniform cells) [1] [2]. However, when dealing with heterogeneous structures, this rule of thumb can be misleading [3]. One should note that, as the computational domain becomes more complex and more heterogeneous, several higher order modes appear around discontinuities, leading to rapidly varying EM-fields in the spatial directions [3]. The correct capturing and spatial representing of these modes is crucial for the accuracy of the simulation results. Therefore, whenever there is a discontinuity (e.g., changing in constitutive parameters) a sufficiently fine mesh in that region and its neighborhood is required [3]. The question that arise is how fine the mesh should be to ensure correct simulations. As an empirical tradition, every dimension inside the computational domain (even the very small ones) should be discretized into three or more cells. However, this new rule of thumb for discretizing heterogeneous computational domains lacks theoretical basis, and does not rigorously ensure convergence and correctness of results. The reason is that we do not know in advance how fast EM-fields will vary in the presence of such discontinuities.

As a practical solution to this mathematical open-problem, researchers have been using three-techniques to guarantee the accuracy of simulations, namely:

- *Convergence tests*: by a progressive, mesh refinement of the computational domain, until the simulation outcomes remain practically unchanged [4].
- *Mesh adaptation*: EM-fields are evaluated after the every simulation process; then, the mesh is locally refined in regions where rapid field spatial variations are observed. The simulation is then repeated. The procedure is repeated until the results remain practically unchanged [4].
- *Cross verification*: by re-simulating the same problem using different numerical techniques [4].

As a general practice, one should pay attention to the three main sources of error in numerical simulations (due to discretization), namely [3]:

- *Geometrical discretization error*: the difference between real dimensions in continues (real) domain and the ones in the discrete counterpart [3].
- *Numerical dispersion error*: the difference in phase velocity in discrete domain and the continuous one. This type of error is accumulative in spatial directions, rendering it more visible in huge computational problems, where signals travel large distances. This might leads to significant phase error, hence, wrong simulation results. Therefore, one should keep in mind that a tolerable dispersion error depends on the size of the computational domain and it is not merely local phenomenon [3].
- *Coarseness error*: occurs when the mesh is too coarse in regions with rapidly changing EM-fields [3].

Numerical dosimetry -which is the computation of SAR in different tissues using CEM methods- [5]-[13], is a typical category of problems that combine all the previously mentioned sources of error. Moreover, as the frequency increases, the electrical-size of the numerical domain increases too (e.g., at 30 GHz, the wavelength is 10 mm in free-space and 1.5 mm in some human tissues [14]), however, the physical size of the human body remain unchanged. Therefore, it is of crucial importance to be as efficient as possible in meshing such domains. For instance, the simulation of the human head (e.g., $20 \times 20 \times 30$ cm^3) at 30 GHz requires 3.5 billion cells with ($\lambda/10$) mesh-size. A

convergence test with $(\lambda/20)$ mesh-size for instance, will increase the computational domain to 28 billion cells, and a CPU-time16-folds as compared to the previous case.

The main contribution of this article is to study the impact of mesh-size on the simulated SAR results (per cell, and averaged over a certain mass) in strongly heterogeneous environments. Moreover, the impact of tissues EM-properties uncertainty is discussed. In all numerical experiments, comparison between FIT (CST commercial EM-Solver [15]) and TLM methods are presented.

II. Problem Description and Numerical Tools

A. Problem Description

Consider the computational domain shown in fig.1; the domain is decomposed into several homogenous sub-domains Ω_i. The goal is to compute the SAR inside the biological body. The media properties in any tissue can be mathematically described as:

$$\varepsilon_r(\Omega_i) = \varepsilon_{r,i} \tag{1.a}$$

$$\sigma(\Omega_i) = \sigma_i \tag{1.b}$$

where ε_r is the permittivity, and σ is the electric conductivity. Note that, the biological body (BD) is defined as the union of all its non-overlapping sub-regions Ω_i's:

$$BD = \bigcup_{i=1}^{N} \Omega_i \tag{2}$$

Moreover, the EM-parameters anywhere in BD can be defined as:

$$\varepsilon_r(x,y,z) = \sum_{i=1}^{N} \varepsilon_{r,i}\psi_i(x,y,z) \tag{3.a}$$

$$\sigma(x,y,z) = \sum_{i=1}^{N} \sigma_i\psi_i(x,y,z) \tag{3.b}$$

where the shape-function $\psi_i(x,y,z)$ is defined as:

$$\psi_i(x,y,z) = \begin{cases} 1, & if\ (x,y,z) \in \Omega_i \\ 0, & Otherwise \end{cases} \tag{4}$$

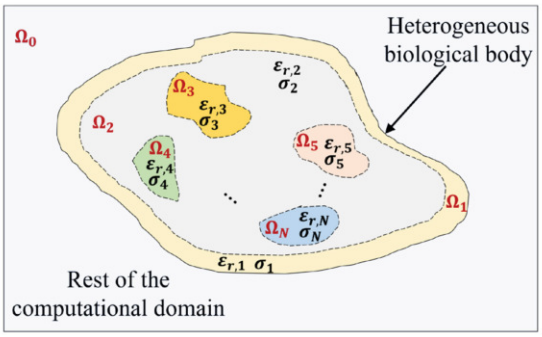

Fig. 1, generic computational domain containing a biological entity, the objective is to compute the SAR in the different tissues, propagating devices and other elements exist in the surrounding environment

The objective now is to find the maximum mesh-size that ensures correct EM-fields distribution; hence, correct SAR levels after discretizing the domain BD.

From the argument presented in the introduction, one can expect that the desired mesh-size will depend on both media properties of different sub-regions and the corresponding shape functions.

The complex permittivity of human tissues at any given angular frequency ω can be expressed in terms of fourth order Cole-Cole model as [14]:

$$\varepsilon = \varepsilon_\infty + \sum_{i=1}^{4} \frac{\Delta\varepsilon_i}{(1+j\omega\tau_i)^{(1-\alpha_i)}} + \frac{\sigma}{j\omega\varepsilon_o} = \varepsilon' + j\varepsilon'' \tag{5}$$

where ε_∞ is the permittivity at very high frequencies, ε_o is the vacuum permittivity, σ the electric conductivity, τ_i, $\alpha_i$and $\Delta\varepsilon_i$ are different parameters used for adjusting the curve fitting model (5) to measurements [14].

In such lossy-dielectric sub-domains, the wavelength can be locally expressed in each Ω_i as:

$$\lambda_i = 2\pi/\beta_i \tag{6.a}$$

where the propagation constant β is defined as [16]:

$$\beta_i = \omega\left\{\frac{\mu_0\varepsilon'_i}{2}\left[\sqrt{1+\left(\frac{\varepsilon''_i}{\varepsilon'_i}\right)^2}+1\right]\right\}^{1/2} \tag{6.b}$$

The proposed discretization strategy depends on three factors:

- *Limit 1: numerical dispersion error*

To ensure a negligible numerical dispersion error per cell, the mesh-size should respect the condition [1] [2]:

$$\Delta x \le \frac{1}{10}\min_{1\le i\le N}(\lambda_i) \tag{7}$$

- *Limit 2: geometric discretization error*

Assuming we have the 3D discretization operator $\mathfrak{D}$ that converts any Ω_i (or its corresponding shape function ψ_i) into a discrete 3D geometry. Without loss of generality we will assume the resulting 3D geometries as structured meshes composed of uniform cubic cells of mesh-size Δx, so:

$$\mathfrak{D}\{\psi_i, \Delta x\} = \tilde{\psi}_i \tag{8.a}$$

Assuming the 3D-shape similarity operator $\boldsymbol{\mathcal{S}}$ gives the similarity factor ξ between any two shape-functions, say, ψ_i and $\tilde{\psi}_i$:

$$\xi_i = \boldsymbol{\mathcal{S}}\{\psi_i, \tilde{\psi}_i\} \tag{8.b}$$

where $0 \le \xi_i \le 1$, the higher ξ_i the better the resemblance is between the discrete sub-domain and the corresponding continues one. Therefore, one should choose a mesh-size Δx that guarantee a similarity factor over a certain threshold value ξ_{th} (e.g., $\xi_{th} = 95\%$). In other words, the goal is to maximize the mesh-size with the constraint $\xi_i \ge \xi_{th}$ in all sub-domains:

$$\max_{\substack{\xi_i \ge \xi_{th} \\ 1\le i\le N}} \Delta x \tag{8.c}$$

Keeping in mind that the similarity factor is not a monotonically increasing function, as the mesh gets finer. However, it tends to increase, as the mesh-size gets smaller.

In literature, one finds several discretizing operators $\mathfrak{D}$ and several metrics $\boldsymbol{\mathcal{S}}$ for similarity between 3D objects [17].

- *Limit 3: coarseness error*

From the theory of EM-waves propagation in heterogeneous media, it is well known that fields are interrupted when they

encounter a change in media properties. This interruption is usually observed around critical regions, such as for instance, sharp edges, corners, slots, fine-details…etc [3].

Coming back to the description of our model in continues media in (3). The objective is to find the maximum mesh-size that guarantees correct fields' spatial description, especially in critical regions and their neighborhoods.

Based on the geometrical characteristics of every shape functions ψ_i, its media properties, media properties of the adjacent sub-domains. Empirically, it was observed that the finest detail should be discretized into several cells to obtain correct results. For instance, to obtain the correct input impedance of thin-wire antenna, the circular cross section should be discretized into at least 20 cells. However, for the SAR computations, it is sufficient to discretize the smallest dimension into three cells using the TLM method. On the other hand, the FIT method might need more cells to reach convergence, as we will see in the next section.

It is worth mentioning that, the Virtual Population (ViP) - developed in IT'IS foundation- provides Computer Aided Design (CAD) description of human models with their different organs [14]. Therefore, one can generate voxel-based human phantoms as fine as needed from these CAD models (ViP2.x and above) [14].

B. Numerical Schemes

Several numerical schemes are used in literature for numerical dosimetry applications including time-domain methods such as the Finite-Difference Time-Domain method (FDTD) [5] [9] [11], Discontinuous Galerkin Time-Domain method (DGTD) [7], FIT [12] [13] and TLM [6] [13] [18] [19], and Frequency-Domain methods, such as the Finite Elements Method (FEM) [10]. Note that for hexahedral cells both FIT and FDTD methods have similar numerical behavior and properties. In the results section, comparisons between FIT and TLM methods are presented. However, it is worth mentioning that both methods have different origins and work differently. The FIT (based on direct discretization of Maxwell's equations in their integral form); therefore, an averaging process in media properties is necessary at the interface between different media [12]. However, the TLM method (based on the analogy between Maxwell's equations and circuit theory) represent the computational domain into 3D cells interconnected via a network of transmission lines, and the interaction between media and EM-fields occurs at the cells' centers [18] [19] [20]. Therefore, no averaging at the interface between different media is required.

III. RESULTS AND DISCUSSIONS

In this section, two experiments are presented to study the behavior of convergence speed in SAR computation using both FIT and TLM methods, for both local per cell SAR distribution, and the averaged SAR over a specific mass. The first example considers a very heterogeneous structure (3D periodic structure composed of two lossy-dielectric media). This heterogeneity plays a significant role in decelerating the convergence, especially for the FIT method. The second experiment is multi-layered sphere of different lossy-dielectrics (skin, fat, muscles, bone, and brain). This structure is less heterogeneous as compared to the previous one. A third experiment is presented to study the impact of uncertainty in constitutive parameters on both the local and the averaged SAR distributions. All TLM simulations are conducted using an in-house-built EM parallel solver.

A. SAR Distribution in a 3D Periodic Structure of Lossy Dielectric Media

In this experiment, the cube shown in fig.2 below is illuminated by a plane-wave (propagation in $+z$ direction, polarization along x-axis). The goal is to compute the SAR distribution everywhere inside the cube at the frequency 4.2 GHz.

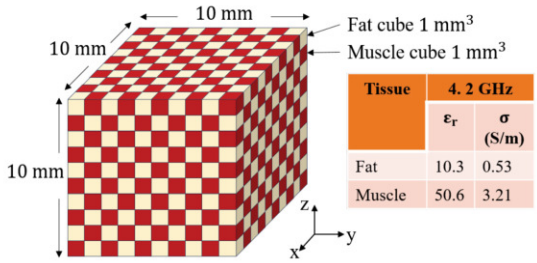

Tissue	4. 2 GHz	
	ε_r	σ (S/m)
Fat	10.3	0.53
Muscle	50.6	3.21

Fig. 2, dielectric cube composed of fat and muscle small cubes, excited by a plane-wave.

Different mesh-sizes are used to discretize the structure. Starting from $\Delta x = 1$ mm or ($\Delta x \approx \lambda_{min}/10$), the mesh use continuously refined until $\Delta x = 0.1$ mm or ($\Delta x \approx \lambda_{min}/96$). The time-domain excitation signal is a modulated Gaussian-pulse of parameters ($f_0 = 4.2$ GHz, $t_0 = 3.32$ ns, $\sigma = 664$ ps). Huygens's box is used to generate the plane-wave excitation, and a PML layer is used as an absorbing boundary condition. The SAR values are renormalized to an incident power of 120 Watt at 4.2 GHz.

Fig.3 and fig.4 show the SAR distributions averaged over 20 mg, obtained using TLM and FIT methods, respectively. One can notice practically similar distributions are obtained using TLM with 38 cells per wavelength or finer. However, using the FIT method one needs 76 cells or finer to obtain convergence.

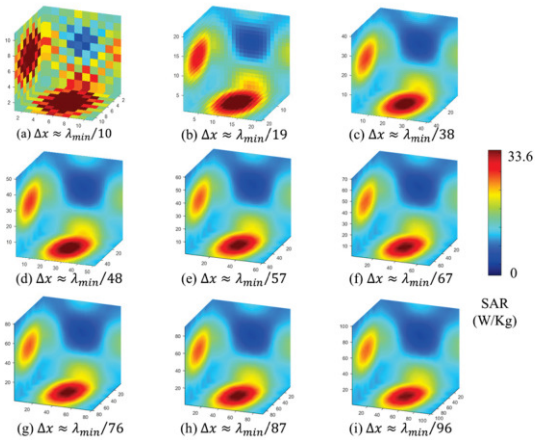

Fig. 3, TLM SAR distributions (averaged over 20 mg of tissues).

Table I shows the maximum SAR levels for both averaged and non-averaged (per cell raw SAR results). One can observe that the TLM converges faster than the FIT method.

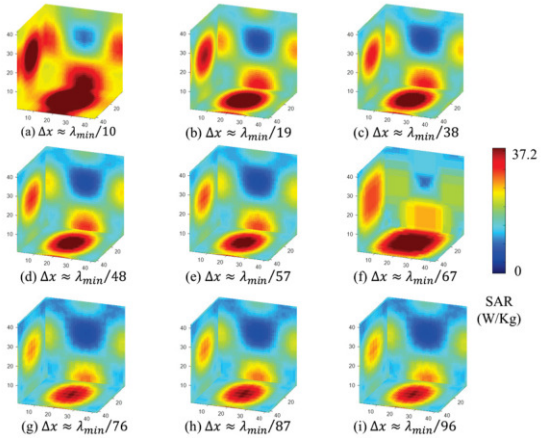

Fig. 4, FIT (CST Software) SAR distributions (averaging over 20 mg of tissues). Different discretization levels.

The averaged SAR values over a certain mass are obtained using an algorithm developed in [11]. This post-processing algorithm has a relatively high computational complexity. If we consider the memory' complexity of the computational domain is $O(N^3)$ then the time complexity of the SAR averaging algorithm is $O(N^6)$, where $N \sim$ cubic root of the number of cells in the computational domain.

TABLE I. MAXIMUM SAR VALUES (PER CELL AND AVERAGED) FOR BOTH TLM AND FIT AT DIFFERENT DISCRITIZATION Δx

	FIT Method		TLM Method	
Mesh-size Δx	**SAR max per cell (W/Kg)**	**SAR 20 mg max (W/Kg)**	**SAR max per cell (W/Kg)**	**SAR 20 mg max (W/Kg)**
λ/10	60.2	58.965	103.9	71.47
λ/19	103.1	46.4	63.2	39.26
λ/38	164.1	44.5	72.8	35.42
λ/48	188.2	42.2	81.9	35.7
λ/57	225.4	40.6	85.8	34.3
λ/67	251.9	39.5	96.7	33.9
λ/76	289.8	38.5	107.7	34.2
λ/86	317.3	37.8	120.4	34.4
λ/96	345.2	37.2	127.6	33.6

B. SAR distribution in Lossy-Dielectric Concentric Spheres

The sphere shown in fig.5 is a simplified model of the human head composed of five layers of tissues. Huygens's box is used to excite the sphere by a plane-wave (propagation in $+x$ direction, polarization along z-axis). Different mesh-sizes are used to discretize the structure. Starting from $\Delta x =$ 1 mm or ($\Delta x \approx \lambda_{min}/12$), the mesh use continuously refined until $\Delta x = 0.2$ mm or ($\Delta x \approx \lambda_{min}/60$). The time-domain excitation signal is a modulated Gaussian-pulse of parameters $t_0 = 3.32$ ns, $\sigma = 664$ ps, the center frequency $f_0 = 3.5$ and 6 GHz, respectively. All SAR values are renormalized to an incident power of 200 Watt at 3.5GHz, and 6 GHz, respectively.

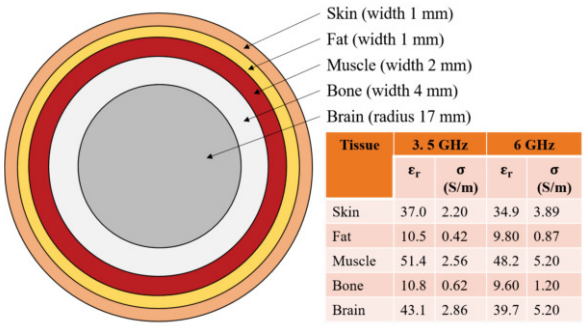

Tissue	3. 5 GHz		6 GHz	
	ε_r	σ (S/m)	ε_r	σ (S/m)
Skin	37.0	2.20	34.9	3.89
Fat	10.5	0.42	9.80	0.87
Muscle	51.4	2.56	48.2	5.20
Bone	10.8	0.62	9.60	1.20
Brain	43.1	2.86	39.7	5.20

Fig. 5, multi-layered sphere of different human head tissues.

Fig.6 and fig.7 show the 1g averaged SAR distributions on the sphere's surface at 3.5 and 6 GHz frequencies, respectively. Good matching in 1g averaged SAR distribution is observed between FIT and TLM methods at both frequencies. Tables II and III show also a good matching in the maximum SAR for both TLM and FIT methods.

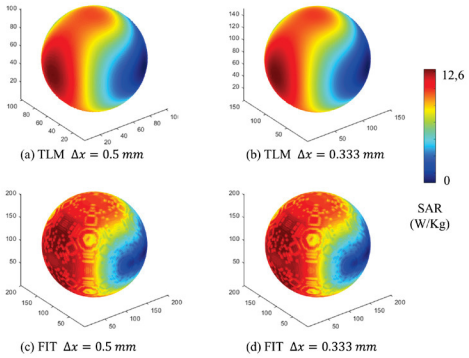

Fig. 6, SAR distributions (averaging over 1 g of tissues) at 3.5 GHz, FIT (CST Software) vs. TLM methods for different discretization levels.

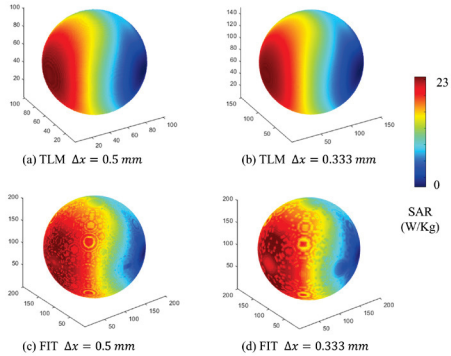

Fig. 7, SAR distributions (averaging over 1 g of tissues) at 6 GHz, FIT (CST Software) vs. TLM methods for different discretization levels.

TABLE II. MAXIMUM SAR VALUE (AVERAGED AND PER CELL) FOR DIFFERENT DISCFRETIZATIONS. TLM METHOD.

Mesh-size Δx	**3.5 GHz**		**6 GHz**	
	SAR per cell (W/Kg)	**SAR 1 g (W/Kg)**	**SAR per cell (W/Kg)**	**SAR 1 g (W/Kg)**
1 mm	33.7	14.3	-	-
0.5 mm	32.4	13.7	99.5	22.98
1/3 mm	32.2	13.56	104.2	23.24
0.2 mm	32.1	13.63	103.9	23.13

TABLE III. MAXIMUM SAR VALUE (AVERAGED AND PER CELL) FOR DIFFERENT DISCFRETIZATIONS. FIT METHOD.

Mesh-size Δx	3.5 GHz		6 GHz	
	SAR per cell (W/Kg)	SAR 1 g (W/Kg)	SAR per cell (W/Kg)	SAR 1g (W/Kg)
1 mm	27.5	11.96	-	-
0.5 mm	30.1	12.38	98.85	23.29
1/3 mm	31.3	12.61	106.22	23.00
0.2 mm	31.5	12.63	112.76	23.04

C. Imact of Uncertaininty in Tissues Parameters on SAR Levels (multi-layerd sphere model)

A similar setup is used as in the previous experiment (fig. 5), however, the tissues constitute parameters were increased by 1%, 5% and 10% consecutively. The objective is to show the impact of uncertainty in these parameters on the SAR distribution.

As shown in table IV below, the SAR levels vary for both the SAR per cell and the averaged SAR as a function of the perturbation in the constitutive parameters.

TABLE IV. MAXIMUM SAR VALUE (AVERAGED AND PER CELL) FOR DIFFERENT VALUES OF $(\varepsilon_r$ AND $\sigma)$ FOR THE MULTI-LAYERED SPHERE IN FIG.5.

Permittivity & conductivity	Original values (fig. 5)	+1%	+5%	+10%
SAR per cell max (W/Kg)	31.3	31.1	30.4	29.7
SAR 1g max (W/Kg)	12.6	12.5	11.9	11.3

IV. CONCLUSION

As the operating frequencies increase the electric size of the human model proportionally increases. This leads to bigger computational problems. Moreover, the high heterogeneity of the human body tissues properties plays an important role in choosing the necessary mesh-size that guarantees convergent results (hence, accurate ones). As a general role, it is necessary to reduce the mesh-size as the heterogeneity of the computational domain increases. The TLM methods shows a faster convergence in SAR computations at sub-6 GHz 5G frequency bands as compared to FIT method. This faster convergence was also observed at LF and VLF frequencies in previous publications. The averaged SAR over a certain mass converges faster than the local SAR per cell. Finally, the uncertainty in tissues properties has an important impact on both local and averaged SAR levels.

ACKNOWLEDGMENT

This work benefited from access to CINES computing resources through the 2021 A0100505122 resource allocation attributed by GENCI.

REFERENCES

[1] A. A. Ijjeh, M. M. N. Ney, and F. P. Andriulli, “Stability and dispersion analysis of a TLM unified approach for dispersive anisotropic media,” IEEE Trans. Microw. Theory Techn., vol. 65, no. 4, pp. 1141–1149, Apr. 2017.

[2] A. Taflove, S. C Hagness and M. Piket-May, Computational electromagnetics: the finite-difference time-domain method. The Electrical Engineering Handbook, 3. (2005).

[3] A. A. Ijjeh, M. Cueille, J. -L. Dubard and M. M. Ney, "Dispersion and Stability Analysis for TLM Unstructured Block Meshing," in IEEE Transactions on Microwave Theory and Techniques, vol. 69, no. 10, pp. 4352-4365, Oct. 2021, doi: 10.1109/TMTT.2021.3093417.

[4] T. Weiland, M. Timm and I. Munteanu, "A practical guide to 3-D simulation," in IEEE Microwave Magazine, vol. 9, no. 6, pp. 62-75, December 2008, doi: 10.1109/MMM.2008.929772.

[5] J. Shi, J. Chakarothai, J. Wang, O. Fujiwara, K. Wake and S. Watanabe, "Improvement of SAR Accuracy by Combining Two SAR Quantification Methods for Small Animals in Reverberation Chamber Above 10 GHz," in IEEE Access, vol. 8, pp. 138170-138178, 2020, doi: 10.1109/ACCESS.2020.3011830.

[6] A. Ijjeh, et al. "Numerical dosimetry in human model for 5G and beyond." Union Radio-Scientifique Internationale (URSI-FRANCE 2020 WORKSHOP). 2020.

[7] Descombes, S., Lanteri, S., & Moya, L. (2016). Locally implicit discontinuous Galerkin time domain method for electromagnetic wave propagation in dispersive media applied to numerical dosimetry in biological tissues. SIAM Journal on Scientific Computing, 38(5), A2611-A2633.

[8] International Commission on Non-Ionizing Radiation Protection (2020). Guidelines on limiting exposure to electromagnetic fields (100 kHz to 300 GHz)”. Health Physics 118:483–524.

[9] A. D. Tinniswood, C. M. Furse and O. P. Gandhi, "Computations of SAR distributions for two anatomically based models of the human head using CAD files of commercial telephones and the parallelized FDTD code," in IEEE Transactions on Antennas and Propagation, vol. 46, no. 6, pp. 829-833, June 1998, doi: 10.1109/8.686769.

[10] A. Citkaya and S. Seker. "FEM modeling of SAR distribution and temperature increase in human brain from RF exposure." International Journal of Communication Systems 25.11 (2012): 1450-1464.

[11] K. Caputa, M. Okoniewski and M. A. Stuchly, "An algorithm for computations of the power deposition in human tissue," in IEEE Antennas and Propagation Magazine, vol. 41, no. 4, pp. 102-107, Aug. 1999, doi: 10.1109/74.789742.

[12] E. Gjonaj, M. Bartsch, M. Clemens, S. Schupp and T. Weiland, "High-resolution human anatomy models for advanced electromagnetic field computations," in IEEE Transactions on Magnetics, vol. 38, no. 2, pp. 357-360, March 2002, doi: 10.1109/20.996096.

[13] Laisné, Alexandre, and Julien Drouet. "Comparison of finite integration technique (fit) and transmission line matrix (tlm) for numerical dosimetry in hf/vhf band." Electromagnetic Compatibility (EMC EUROPE), 2013 International Symposium on. IEEE, 2013.

[14] https://itis.swiss/virtual-population

[15] https://www.3ds.com/fr/produits-et-services/simulia/produits/cst-studio-suite/

[16] J-D. Jackson. Classical electrodynamics. 1999.

[17] J. L. Mari, F. Hétroy-Wheeler and & G. Subsol. Geometric and Topological Mesh Feature Extraction for 3D Shape Analysis. John Wiley & Sons. 2020.

[18] Johns, Peter B. "A symmetrical condensed node for the TLM method." IEEE Transactions on Microwave Theory Techniques 35 (1987): 370-377.

[19] C. Christopoulos, The Transmission-Line Modeling (TLM) Method in Electromagnetics of Synthesis Lectures on Computational Electromagnetics, San Mateo, CA, USA:Morgan Kaufmann, pp. 65-121, 2006.

[20] A. Ijjeh, M. M. Ney, and F. Andriulli. "Behavior of Time-Domain volumic methods in presence of high-contrast media or irregular structured mesh interfaces." 2015 9th European Conference on Antennas and Propagation (EuCAP). IEEE, 2015.